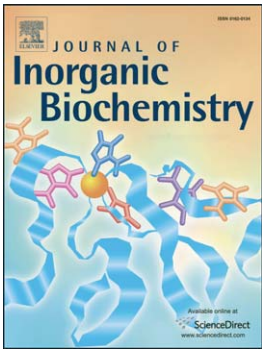

pH-metric chemical speciation modeling and studies of *in vitro* antidiabetic effects of *bis*[(imidazolyl)carboxylato]oxidovanadium(IV) complexes

Isaac Z. Gundhla, Ryan S. Walmsley, Vital Ugirinema, Nandipha O. Mnonopi, Eric Hosten, Richard Betz, Carminita L. Frost, Zenixole R. Tshentu

PII: S0162-0134(14)00312-2
DOI: doi: 10.1016/j.jinorgbio.2014.12.019
Reference: JIB 9642

To appear in: *Journal of Inorganic Biochemistry*

Received date: 25 March 2014
Revised date: 18 December 2014
Accepted date: 19 December 2014

Please cite this article as: Isaac Z. Gundhla, Ryan S. Walmsley, Vital Ugirinema, Nandipha O. Mnonopi, Eric Hosten, Richard Betz, Carminita L. Frost, Zenixole R. Tshentu, pH-metric chemical speciation modeling and studies of *in vitro* antidiabetic effects of *bis*[(imidazolyl)carboxylato]oxidovanadium(IV) complexes, *Journal of Inorganic Biochemistry* (2014), doi: 10.1016/j.jinorgbio.2014.12.019

pH-metric chemical speciation modeling and studies of *in vitro* antidiabetic effects of *bis*[(imidazolyl)carboxylato]oxidovanadium(IV) complexes

Isaac Z. Gundhla,[a] *Ryan S. Walmsley,*[a] *Vital Ugirinema,*[b] *Nandipha O. Mnonopi,*[c] *Eric Hosten,*[b] *Richard Betz,*[b] *Carminita L. Frost,*[c,*] *Zenixole R. Tshentu*[b,*]

[a]Department of Chemistry, Rhodes University, P.O. Box 94, Grahamstown 6140, South Africa

[b]Department of Chemistry, Nelson Mandela Metropolitan University, P.O. Box 77000, Port Elizabeth 6031, South Africa

[c]Department of Biochemistry and Microbiology, Nelson Mandela Metropolitan University, P.O. Box 77000, Port Elizabeth 6031, South Africa

Abstract

A range of bidentate N,O-donor ligands of the imidazolyl-carboxylate moiety, which partially mimic naturally occurring bioligands, were prepared and reacted with the oxidovanadium(IV) ion to form the corresponding *bis*-coordinated oxidovanadium(IV) complexes. The aqueous pH-metric chemical speciation was investigated using glass electrode potentiometry which allowed for the determination of protonation and stability constants of the ligands and complexes, respectively. The species distribution diagrams generated from this information gave evidence that the *bis*[(imidazolyl)carboxylato]oxovanadium(IV) complexes possess a broad pH-metric stability. The complexes improved glucose uptake in cell cultures using 3T3-L1 adipocytes, C2C12 muscle cells and Chang liver cells. The PTP inhibition studies indicated that the mechanism underlying insulin-stimulated glucose uptake was possibly *via* the protein tyrosine phosphorylation through inhibition of the protein tyrosine phosphatase 1B (PTP 1B). The vanadium compounds also demonstrated the inhibition of D-dimer formation, suggesting that these compounds could potentially relieve a hypercoagulative state in diabetic patients.

Keywords: oxidovanadium(IV) complexes, speciation, anti-diabetic effects, anti-coagulative effects

* Emails: carminita.frost@nmmu.ac.za (C.L. Frost) and zenixole.tshentu@nmmu.ac.za (Z.R. Tshentu)

1. Introduction

Diabetes mellitus, a chronic metabolic disorder, is becoming a major health concern worldwide, and the cost of treatment for this burden is becoming an insurmountable undertaking for low and middle-income countries [1,2]. Insulin, a pancreatic signaling hormone, is the principal treatment for type 1 diabetes while type 2 diabetes can often be controlled by oral pharmaceuticals namely; sulphonylureas such as glipizide, biguanides such as metformin, thiazolidinediones such as pioglitazone, and meglitinides such as prandin. However, these available prescription drugs present adverse side effects including hypoglycaemia for sulphonylureas, lactic acidosis for the biguanides, and weight gain for thiazolidinediones. Therefore, there is a need for the development of another class of oral pharmaceuticals that does not present undesirable side effects, and vanadium has shown promise in this regard.

Vanadium is by no means the only metal that has therapeutic effects for the treatment of diabetes mellitus. Metals or minerals such as copper, manganese, zinc and selenium exhibit increased sensitivity to insulin due to their ability to relieve the oxidative stress caused by the reactive oxygen species within cells [3,4]. At high doses, however, these metals may become pro-oxidant hence supplementation is often restricted to a change of diet to include foods richer in minerals. The supposed positive role of chromium in glucose metabolism has also resulted in the marketing of chromium as a nutritional supplement with chromium picolinate being available over the counter in a form of pills, sports drinks and nutrition bars [4]. However, Cefalu *et al*. (2010) have recently carried out a comprehensive study on the metabolic and physiological response from chromium supplementation and suggested that chromium is most likely to elicit a response to insulin resistant individuals who have more elevated fasting glucose [5]. Vanadium compounds are also being considered for mitigating insufficient insulin response in diabetes mellitus [6]. They cannot, however, entirely substitute for lack of insulin (as in type 1 diabetes) but can reduce reliance on exogenous insulin and/or perhaps substitute for other oral hypoglycaemic agents used in treatment of type 2 diabetes [7,8]. Inorganic salts of vanadium have shown promising glucose metabolism

action but the potential toxicity of vanadate (anionic form) and low absorption rate of oxidovanadium(IV) (cationic form) pushed the focus towards designing new organovanadium compounds [9,10]. Thus tailoring of the properties of these vanadium complexes can be achieved by simple modification of the organic ligand.

Vanadate and oxidovanadium(IV) are the main species that can exist under physiological conditions [6]. The physiological effects are in many cases a consequence of the good complexation behaviour of the VO^{2+} ion with a carrier ligand, allowing it to be absorbed in a complexed form and then released in the bloodstream to be shuttled by biological ligands such as transferrin to the cells [11]. Vanadium has been implicated in performing many functions of insulin such as inhibition of lipolysis and gluconeogenesis as well as stimulating lipogenesis and cellular glucose uptake, hence its compounds are referred to as insulin-mimetics [12-15]. The true form of the necessary vanadium species under physiological conditions is a subject of much debate but a focal mechanism of action which seems to enjoy a broad consensus is its involvement in the inhibition of phosphatases [12-15]. The action of vanadium at an intracellular cellular level is due to the structural similarity between phosphate and vanadate. This property leads to the inhibition of protein tyrosine phosphatase 1B (PTP 1B) thereby maintaining the signal for glucose internalisation and subsequent metabolism is achieved [16,17]. A few vanadium compounds seem to have insulin-enhancing effects, and among others, *bis*(picolinato)oxidovanadium(IV) has proved to be orally active in treating diabetes mellitus [18], and *bis*(maltolato)oxidovanadium(IV) (BMOV) and *bis*(ethylmaltolato)oxidovanadium(IV) (BEOV) have also shown significant glucose lowering effect [19], with the latter having undergone Phase IIa clinical trials [7].

The development of vanadium anti-diabetic metallo-pharmaceuticals is focused on oral agents for lowering blood glucose levels, therefore the complexes must be thermodynamically stable in both acidic and neutral environments. This stability is required because the vanadium complex must survive the digestion process where the pH can be as low as 2 and must also remain intact under pH conditions of the intestines and be delivered in significant doses into the bloodstream where the pH

can be as high as 7.4. Therefore the determination of the thermodynamic stability of the vanadium complexes as a function of pH is a necessary prerequisite for evaluating the usefulness of such complexes to serve as glucose-lowering drugs. The ligands, therefore, act as shields that help to stabilize vanadium complexes under the pH conditions of the digestive tract and intestines, and assist with absorption of vanadium into the bloodstream. The latter renders the balance of hydrophilicity and hydrophobicity of the complexes very important [19]. The pH-metric chemical speciation of the vanadium compounds can be appropriately designed through the correct combination of donor atoms involved in the bidentate coordination of the ligands in order to achieve the requisite stabilization under the physiological pH range.

This study explores the use of imidazole derivatives as binding moiety to oxidovanadium(IV) since imidazoles are known to play a significant role in a large variety of biological processes [20]. We have shown that imidazolyl-carboxylates are simple and effective bidentate ligands for stabilizing $V^{IV}O$ in biological systems. The syntheses and characterization of the oxidovanadium(IV) complexes with imidazole-4-carboxylic acid (Im4COOH), imidazole-2-carboxylic acid ((Im2COOH) and 1-methylimidazole-2-carboxylic acid (MeIm2COOH) as coordinating ligands is presented. The stability constants for the complexation of oxidovanadium(IV) to the ligands were determined *via* potentiometric acid-base titrations. The anti-diabetic potential of these complexes has been investigated *via* the *in vitro* glucose assay using 3T3-L1 adipocytes, C2C12 muscle cells and Chang liver cells as well as the PTP 1B inhibition assay. In addition, both the extrinsic and intrinsic coagulation pathways [21,22] were investigated in order to ascertain the potential of the complexes in relieving blood coagulation.

2. Experimental Section

2.1 Materials and instrumentation

Oxidovanadium(IV) sulfate hydrate was obtained from BDH Limited (England). 1-Methylimidazole (MeIm) (99%) and Im4COOH (**1a**) (98%) were obtained from Sigma-Aldrich (USA). Imidazole-2-carboxaldehyde (97%) was obtained from Fluka (USA). All solvents were

obtained from Merck Chemicals (SA) and were of reagent grade and used without further purification. Other reagent grade chemicals were also obtained from commercial sources and used as received. PTP 1B was purchased from Sigma-Aldrich (SA) and microtiter plates from Lasec (SA).

The infrared spectra were recorded on a Perkin Elmer 2000 FTIR spectrometer in the mid-IR range (4000 – 400 cm^{-1}) as KBr pellets. ^{1}H and ^{13}C NMR spectra of all ligands were recorded on a Bruker AMX 400 NMR MHz spectrometer and reported relative to tetramethylsilane (δ 0.00). Electronic spectra were recorded on a Perkin Elmer Lambda 25 UV-Vis spectrophotometer using 1 cm quartz cells and water as the solvent. Microanalysis was carried out using a Vario Elementar Microcube ELIII. Potentiometric studies were performed using a Metrohm 794 Titrino equipped with a Metrohm LL Ecotrode. A Bio-Tek KC4 powerwave XS microtiter plate reader was used to measure absorbance for 3-(4,5-dimethylthiazol-2-yl)-2,5-diphenyl tetrazolium bromide (MTT), Glucose and PTP 1B inhibition assays.

2.2 Preparative work

2.2.1 Im2COOH (1b)

An aqueous 30% H_2O_2 solution (10 g) was added dropwise to a stirred solution of imidazole-2-carboxaldehyde (2.88 g 0.030 mol) in water (10 ml). The reaction was allowed to proceed at room temperature for 72 h, following which the water was removed *in vacuo* at room temperature to afford a white crystalline solid. This solid was washed with a stirred mixture of diethylether/water (4:1) to remove the excess peroxide. Note: heating causes decarboxylation. Yield: 97.5%. Mp = 156-158^{o}C. δ_H (400 MHz, D_2O): 7.56 (2H, s, Im-H); δ_C (400 MHz, D_2O): 158.86, 141.02, 120.49 ppm. IR ν (KBr): 3392(m), 3124(m), 2861(m), 1618(s), 1502(m), 1462(m), 1421(s), 1388(s), 1322(m), 1108(s), 925(s), 910(s), 819(m), 797(s), 774(m) cm^{-1}. *Anal*. Calc. for $C_4H_6N_2O_3$ (130.11); C, 36.92; H, 4.65; N, 21.53%. Found: C, 37.18; H, 4.94; N, 21.47%.

2.2.2 MeIm2COOH (1c)

Firstly, 1-methylimidazole-2-carboxaldehyde was prepared according to the literature procedure [23]. The synthesis procedure then followed that of Im2COOH (**1b**) above and the yield was also quantitative after the removal of water under high vacuum (no washing with diethylether/water was necessary). Note: heating causes decarboxylation. Yield: 100%. Mp = 99-101^{o}C. δ_H (400 MHz, D_2O): 7.42, 7.39 (2H, s, Im-H) and 4.08 ppm (3H, s, NCH_3); δ_C (400 MHz, D_2O): 158.67, 139.68, 125.83, 118.46, 36.73 ppm. IR ν (KBr): 3347(m) 3119(m), 2663(w), 1641(s), 1683(m), 1507(s), 1449(m), 1388(s), 1338(s), 1285(s), 1173(m), 1123(s), 961(m) 910(m), 776(s), 685(s) cm^{-1}. *Anal*. Calc. for $C_5H_8N_2O_3$ (144.12); C, 41.67; H, 5.59; N, 19.44%. Found: C, 41.28; H, 5.23; N, 19.12%.

2.2.3 $VO(im4COO)_2.H_2O$ (2a)

This complex was prepared according to a literature method but with slight modifications [24]. To a stirred aqueous solution of Im4COOH (0.254 g, 2.26 mmol), was added 10% TMAOH (1.13 mmol). To this solution was added aqueous $VOCl_2$ (1.13 mmol), prepared by the reaction of $VOSO_4$ with $BaCl_2$. The reaction was allowed to stir overnight, following which the light blue precipitate was collected, washed with methanol and ether and dried in an oven (100^{o}C). Yield: 64.6%. Mp>300ºC. IR ν (neat): 3129(m), 2992(m), 2856(m), 1606(s), 1573(s), 1499(m), 1439(m), 1356(s), 1209(m), 1080(m), 1012(m), 981(s), 878(m), 819(s), 780(s) cm^{-1}. *Anal*. Calc. for $C_8H_8N_4O_6V$ (307.11); C, 31.29; H, 2.63; N, 18.24%. Found: C, 31.20; H, 2.67; N, 18.14%. UV/Vis (solid reflectance) λ_{max} (nm): 733, 593, 346.

2.2.4 $VO(im2COO)_2.H_2O$ (2b)

This complex was prepared in the same manner as **2a,** except that an aqueous solution of $VOSO_4$ was added to the ligand solution instead of aqueous $VOCl_2$. Yield: 69.9%. Mp > 300ºC. IR ν (neat): 3448(m), 3129(w), 3008(m), 2906(m), 1625(s), 1558(m), 1487(m), 1398(s), 1338(m), 1277(m), 1171(m), 1112(s), 984(s), 908(m), 829(m), 769(s), 658(s) cm^{-1}. *Anal*. Calc. for $C_8H_8N_4O_6V$

(307.11); C, 31.29; H, 2.63; N, 18.24%. Found: C, 31.21; H, 2.53; N, 18.07%. UV/Vis (solid reflectance) λ_{max} (nm): 744, 592, 338.

2.2.5 VO(MeIm2COO)$_2$.H$_2$O (2c)

This complex was prepared similarly to **2a**. However, upon stirring overnight a blue precipitate did not form. The blue solution was then allowed to stand for 24 h and a light blue precipitate formed, which was filtered and washed with methanol and then ether and dried in an oven at 100 ^{o}C. Yield 62.3%. Mp = 218-220ºC. IR ν (neat): 3134 (m), 1628(s), 1487(s), 1426(s), 1327(s), 1286(m), 1180(s), 1166(s), 963(s), 837(m), 797(s), 769(s), 698(s) cm^{-1}. *Anal*. Calc. for $C_{10}H_{12}N_4O_6V$ (335.17); C, 35.83; H, 3.61; N, 16.72%. Found: C, 36.01; H, 3.47; N, 16.67%. UV/Vis (solid reflectance) λ_{max} (nm): 736, 585, 362.

2.3 X-ray structure determination

X-ray diffraction analysis of **VO(im4COO)$_2$·H$_2$O (2a)** was performed at 200 K using a Bruker Kappa Apex II diffractometer with a monochromated Mo Kα radiation (λ = 0.71073 Å). APEXII [25] was used for data collection and SAINT [25] for cell refinement and data reduction. The structure was solved by direct methods using SHELXS–2013 [26] and refined by least-squares procedures using SHELXL-2013 [26] with SHELXLE [27] as a graphical interface. All non-hydrogen atoms were refined anisotropically. Carbon-bound H atoms were placed in calculated positions (C–H 0.95 Å for aromatic carbon atoms) and were included in the refinement in the riding model approximation, with U_{iso}(H) set to 1.2U_{eq}(C). Nitrogen-bound H atoms were located on a difference Fourier map and refined freely. Data were corrected for absorption effects using the numerical method implemented in SADABS [25].

2.4 Potentiometric studies

The protonation and stability constants for the ligands and oxidovanadium(IV) complexes were determined by potentiometric titration of approximately 25 ml samples. All solutions were prepared using freshly boiled and degassed deionized milli-Q water to ensure the removal of dissolved oxygen and carbon dioxide. The ligand concentration was 1 mM and metal-to-ligand ratios of 1:1, 1:5 and 1:10 were used. Titrations were performed over the pH range of 2-11 under a continuous flow of purified nitrogen using HCl and tetramethylammonium hydroxide (TMAOH). The vanadium stock solution containing 0.10 M HCl was standardized by titration with permanganate. The ionic strength of the titration solutions was kept constant at 0.10 M tetramethylammonium chloride (TMACl). Titrations were controlled using Tiamo software, and the titration rate used was 0.01 ml/min and the pausing time was 60 s. The glass electrode was calibrated for a strong acid-base reaction by the Gran-method [28] using the program GLEE [29], to determine the standard potential E^o. The ionic product of water (pKw) of 13.83(1) at 25.0±0.1 ^{o}C in 0.10 M TMACl was used in all calculations [30]. The hydrolysis model of a oxidovanadium(IV) system was included in the model; $[VO(OH)_3]^-$ ($\log\beta_{10-3}$ = -18.0) and $[(VO)_2(OH)_5]^-$ ($\log\beta_{20-5}$ = -22.0), while $[VO(OH)]^+$ ($\log\beta_{10-1}$ = -5.94) and $[(VO)_2(OH)_2]^{2+}$ ($\log\beta_{20-2}$ = -6.95) [31] did not fit. The concentration stability constants $\beta_{pqr} = [M_pL_qH_r]/[M]^p[L]^q[H]^r$ were calculated by using the computer program HYPERQUAD [32].

2.5 In vitro studies

2.5.1 Maintenance of cells lines

3T3-L1 preadipocytes, were maintained in Dulbecco's modified eagle medium (DMEM) supplemented with 10% fetal bovine serum (FBS), while C2C12 mouse skeletal myoblasts and Chang liver cells were maintained in RPMI-1640 medium (Sigma) supplemented with 10% FBS. These were incubated at 37 ^{o}C in a humidified incubator with 5% CO_2. Cells were subcultured at 70% confluence and seeded at a density of 35 000 cells/ml (for 3T3-L1) and 25 000 cells/ml (for Chang and C2C12) in 24-well culture plates.

2.5.2 MTT cytotoxicity studies

Cells were seeded in 24 well plates (Nunc) at densities of 25 000 for C2C12 and Chang liver cells, and 35 000 cells/mL for 3T3-L1. After overnight attachment, the culture medium was replaced with medium containing the test compounds at a range of concentrations (0.5-100 μM). Cells were incubated for 48 h at 37 °C, after which the MTT assay was performed [33].

2.5.3 Glucose uptake studies

The glucose uptake assay was performed using the GLUCOSE (Glu-cinet) kit (BAUER) [34]. Control cells were represented by untreated differentiated fat (3T3-L1), liver (Chang) and undifferentiated muscle (C2C12) cells (Con) incubated in culture media. Positive control cells (Met) were represented by untreated differentiated fat, liver and muscle cells exposed to metformin. Cells were then exposed for 48 h to the test compounds. Thereafter glucose uptake was determined and the cell number was normalized using the MTT assay [33].

2.5.4 PTP inhibition assay

PTP 1B was reconstituted according to the manufacturer's instructions. It was used to establish a standard curve (results not shown) ranging from 40 – 320 mU. A modified method from Zhang *et al.* (2006) [35] was performed in a final volume of 200 µl. Forty microliters of PTP 1B (40 mU) was added to 40 µl of assay buffer (50 mM HEPES, 2 mM EDTA, 3 mM DTT, 100 mM NaCl, pH 7.4). To this 120 µl of pNPP substrate (50 mM) was added and the absorbance was measured every 5 min for 60 min at 405 nm.

2.5.5 Anti-coagulation studies

The effect of the various vanadium compounds on blood coagulation was investigated using a CL Coagulation Analyzer (Beckman). The assays used were the HemosIL® activated partial

thromboplastin time (APTT), prothromin time (PT), Fibrinogen-C (Fib-C), and D-Dimer as per the instructions which can be found on the manufacturers website [36]. The APTT assays were performed by adding the test compounds, positive control or diluent, and APTT reagent to plasma. This was incubated for 3 min at 37 °C followed by addition of $CaCl_2$ to initiate coagulation. PT was performed by incubating PT reagent and treatments followed by the addition of plasma. Fib-C was performed by treating diluted plasma [1:4 (v/v)], incubating, and adding bovine thrombin. D-Dimer was performed by adding treatments and reaction buffer to plasma, hereafter D-Dimer latex reagent was added, the vial was mixed 1-2 times and the agglutination measured. Vanadium compounds were used at 10 μM for the screening assays and 0.01 μM, 0.1 μM, and 10 μM for concentration dependence studies, and the positive control was heparin at 0.1 $U.mL^{-1}$.

2.5.6 Statistical analysis

Error bars indicate the standard error of the mean (SEM) unless specified otherwise (n = 3). The two-tail paired test was used to determine significance of results ($p<0.05$) and ($p<0.01$).

3. Results and discussion

3.1 Synthesis and general considerations

The 1-R-imidazole-2-carboxylic acids were prepared from the corresponding imidazole-2-carboxaldehydes by the hydrogen peroxide facilitated oxidation in water [37,38]. This reaction requires no heating and water was the only by-product of oxidation, making it an environmentally friendly option. The only purification necessary was the removal of residual water *in vacuo*, at room temperature for 1-methylimidazole-2-carboxylic acid yielding a quantitative product but imidazole-2-carboxylic acid crystallized out with a mole equivalent of hydrogen peroxide. This was removed by washing with diethylether to prevent the oxidation of oxidovanadium(IV) to vanadium(V) during the synthesis of the complexes.

The complexes were synthesized by addition of an aqueous oxidovanadium(IV) chloride or

oxidovanadium(IV) sulfate solution to an aqueous solution of the corresponding ligand in a 1:2 molar ratio in the presence of a base [38]. The complexes which precipitated out of solution were easily collected by filtration. The compounds (**2a-c**) are slightly soluble in water and tend to decompose in organic solvents, such as acetonitrile, alcohols and N,N-dimethylformamide (DMF), upon dissolution at elevated temperatures.

3.2 Spectroscopic characterization

In the IR spectra (Figs S1-S3) of the complexes (**2a-c**) there are strong absorption bands at 981, 984 and 963 cm^{-1} respectively, which are assigned to the V=O stretch and are within the range 930-1030 cm^{-1} reported in the literature [39]. In an unsubstituted imidazole ring, the ν(C=N) is usually observed at about 1660 cm^{-1} [40]. The coordination-induced shift of this stretching frequency from 1618-1641 cm^{-1} in the 2-substituted free ligands to 1606-1628 cm^{-1} in the complexes was observed [40,41]. It must be acknowledged that the broad and strong peaks in the region of the ν(C=N) are also a representation of the asymmetric COO^- stretching frequencies (usual range of 1540-1660 cm^{-1}). It has been exhibited that the lower the pK_a value of the acid the higher wavenumber for the $\nu_{as}(COO^-)$ [42], and that seems to also be observed in this work. However, confident assignment was only possible for the spectrum of **2a** since a split peak appeared (1573 and 1606 cm^{-1}) which could be assigned to the ν(C=N) and the $\nu_{as}(COO^-)$ respectively (Fig. S1). In the spectra of **2b** and **2c** (Figs S2 and S3), there was little or no splitting of the peaks but appeared broad and that can be interpreted as a significant overlapping of the two bands. There is also evidence of coordination of the carboxylate group on **2a-2c** as evidenced by the slight shift of the $\nu_{as}(COO^-)$ to lower wavenumbers (Figs S1-S3).

The electronic spectra of **2a-2c** display three low intensity d-d transitions, in the range of 330-1000 nm, which are typical of square-pyramidal oxidovanadium(IV) complexes [43]. The coordination of the sixth ligand to oxidovanadium(IV) does not cause significant shift on spectra of square planar oxidovanadium(IV) complexes in the formation of distorted octahedral complexes.

3.3 X-ray crystal structure

Single crystals of **$VO(im4COO)_2 \cdot H_2O$ (2a)** which were suitable for X-ray analysis were obtained from the mother liquor of this complex upon standing it at room temperature for two weeks. The structure has been reported recently by other researchers [24] but in this account it has been re-determined and the unit cell is presented in a standard form (with a space group of $P2_1/c$ not $P2_1/a$) which gives a slightly different unit cell volume as well as slightly different unit cell dimensions and angles. Table 1 shows the crystallographic and structure refinement data for **$VO(im4COO)_2 \cdot H_2O$** while table 2 contains the selected bond lengths and angles. An ORTEP diagram of **$VO(im4COO)_2 \cdot H_2O$** is presented in Fig. 1.

The structure showed discrete molecules. The molecule has a distorted octahedral geometry with the vanadium atom bound to two bidentate $im4COO^-$ ligands, a terminal oxido, and a water molecule. This connectivity is in contrast to the known square-pyramidal VOL_2 complex with L = imidazole-4-acetic acid [44]. There is evidence of a long V–O bond *trans* to the oxidovanadium(IV) V=O bond. The V=O bond length of 1.587(2) Å falls within the range (1.56-1.66 Å) observed for oxidovanadium(IV) compounds containing the N_2O_2 donor set [45,46].

(Insert Fig.1 here)

(Insert Table 1 here)

(Insert Table 2 here)

3.4 pH-metric speciation studies

The protonation (log *K*) and oxidovanadium(IV) complex formation (log β) constants are listed in Table 3 together with standard deviations. The ligands exhibit two protonation processes in the pH range 2-11 for the carboxylate and imidazole groups respectively. The log K_2 values for the protonation of imidazole in all cases, Im4COOH (6.13), Im2COOH (6.44) and MeIm2COOH

(6.75), are lower than those of free imidazole (6.95) [47] and free MeIm (7.20) [48] respectively. The latter is slightly more basic probably due to the presence of the electron releasing methyl substituent. The low log K_1 values (2.70, 2.72 and 1.29) for Im4COOH, Im2COOH and MeIm2COOH respectively suggest internal hydrogen bonding between the protonated imidazole and a carboxylate. This suggests that these ligands exist in a zwitterion form in an aqueous medium such as that observed for simple amino acids in water. The pyrrole sites in Im4COOH and Im2COOH do not dissociate in the pH range measured.

(Insert Table 3 here)

The proposed interactions of these ligands in aqueous solutions with oxidovanadium(IV) are represented by Scheme 1 below. The ligand Im2COOH shows similar interactions and stability with oxidovanadium(IV) as Im4COOH. The species distribution diagrams, which were generated using the program HYSS [51], are represented by Fig. 2 and Figs S4-S5 (in supplementary information) for the ($V^{IV}O$)-Im4COOH, ($V^{IV}O$)-Im2COOH and the ($V^{IV}O$)-MeIm2COOH systems, respectively.

(Insert Scheme 1 here)

The ligands adopt bidentate chelation. The first binding constants could be calculated with a 1:1 metal-to-ligand ratio and precipitation due to the formation of hydrolysis products was observed for titrations with a 1:2 metal-to-ligand ratio. Extensive $V^{IV}O$ complexation was obtained with a high ligand excess (10-fold), allowing for the determination of the second binding constant. The hydroxido binding ($[VOL_2(OH)]^-$) could not be fitted in these solution chemistry models while the assumption of the binary hydroxyl species $[(VO)_2(OH)_5]^-$ as well as $[VO(OH)_3]^-$ in highly basic solutions fitted well. The fitting of the titration data supports the formation of monomeric $[VOL]^+$ and $[VOL_2]$ species as well as $[VOLH]^{2+}$ for MeIm2COOH. For the MeIm2COOH system,

however, the coordination of a protonated ligand is observed at low pH with log β_{111}=14.85(7). This suggests strong binding and the possibility of a symmetrically chelating carboxylate ion, with the imidazole nitrogen protonated (see Scheme 1). The constant for the bidentate coordination of the carboxylate to $[VO(H_2O)_5]^{2+}$ can be calculated to be 8.10 if the protonation equilibrium (pK_2 = 6.75) is considered in the cumulative association constant of 14.85. The formation of $[VO(MeIm2COOH)]^{2+}$, with the chelating carboxylate, was confirmed by analyzing the titration solution at pH 2.05 with IR spectroscopy (Fig. S6). The presence of a broad band at 1643 cm^{-1} is not conclusive evidence of bidentate coordination since the $\nu_{as}(COO^-)$ could be occluded by the ν(C=N). However, the monodentate coordination of the carboxylate group was proven to be at 1628 $cm^{-1}$for the same ligand interacting with the vanadyl ion. A new peak, however, was also found at 1711 cm^{-1} and this could not be assigned confidently.

(Insert Fig. 2 here)

The overall stability constant for the ($V^{IV}O$)-MeIm2COOH system (log β_{120} =15.49(9)) is far larger than that for Im4COOH system (log β_{12} =11.38(8)) and Im2COOH system (log β_{12} =11.62(6)). This can be explained by the fact that the imidazole nitrogen in MeIm2COOH is more basic. However, the overall stability constant of the ($V^{IV}O$)-Im4COOH and ($V^{IV}O$)-Im2COOH systems are comparable to that of ($V^{IV}O$)-imidazole-4-acetic acid (im-4-acetic acid) (log β_{120} =10.70(1)) [49] and that with mildly basic pyridine nitrogen of picolinic acid (log β_{120} =12.11(2)) [50] intimating that the inclusion of an electron donating group in the 1-position of imidazole is important to effect stability. In addition, six-membered ring chelate formation in the ($V^{IV}O$)-imidazole-4-acetic acid system [49] results in weaker binding compared with five-membered ring systems studied here.

For the formation of the *bis*-coordinated $[VOL_2]$ species, the very acidic carboxylic acid groups interact with VO^{2+} at very low pH and the mildly basic imidazole is able to interact with oxidovanadium(IV) at relatively higher pH. The result is the stabilization of these *bis*-coordinated

oxidovanadium(IV) complexes in the relevant biological pH range. This, therefore, implies that the compounds may survive the digestion process and be delivered in the bloodstream as the neat *bis*-coordinated complexes. However, substitution by bioligands will be possible once the compounds are exposed to the blood plasma matrix.

3.5 Biochemical studies

3.5.1 In vitro glucose uptake studies

The vanadium compounds $[VO(Im4COO)_2]$, $[VO(Im2COO)_2]$, $[VO(MeIm2COO)_2]$ and the simple vanadium salt, $VOSO_4$, showed no cytotoxicity (>80% cell viability) between 0.5- 1 μM in the 3T3-L1, Chang and C2C12 cell lines tested as determined by an MTT-cell viability assay. At concentrations from 10 μM and above, the vanadium compounds proved to be cytotoxic (<80% cell viability) (see Figure S7 in the supplementary information section). Thus, the glucose uptake ability of the vanadium compounds was screened at concentrations of 0.5, 1 and 10 μM. The results for the 1 μM concentrations are presented in Fig. 3, while the results for all concentrations tested can be found in Table S1 (in supplementary information).

(Insert Fig. 3 here)

There were varying effects observed in the 3T3-L1 adipocytes (Fig. 3). Metformin, along with oxidovanadium(IV) sulfate and $[VO(Im2COO)_2]$ improved glucose uptake. However for $[VO(Im4COO)_2]$ and $[VO(MeIm2COO)_2]$, less than basal glucose uptake was observed. For the Chang cells, enhanced glucose uptake was observed for all of the oxidovanadium(IV) compounds besides $[VO(Im2COO)_2]$. In the C2C12 cells, $VOSO_4$ and $[VO(Im4COO)_2]$ enhanced glucose uptake to a level comparable to Metformin. It should be noted that a higher level of increase in the percentage of glucose uptake was expected for metformin within the Chang liver cells as this is where metformin is most effective. The results are, however, significant and the difference in our

earlier findings [52] could be due to biological variation between the various passages numbers of cells used. When higher than 1 μM concentrations of the oxidovanadium(IV) compounds were administered to the cells, the general trend was a slight drop in glucose uptake (Table S1), possibly due to some cytotoxic effects at these conditions.

3.5.2 PTP inhibition studies

The PTP 1B inhibition studies were carried out for the complexes in order to validate mechanistic understanding of the effects of vanadium compounds as insulin-enhancing agents [24,53]. For the compounds tested both Lineweaver-Burk and Dixon plots (Fig. S8) were completed and the K_i values were determined. $VO(Melm2COO)_2$, $VO(im2COO)_2$ and $VOSO_4$ had K_i values of 60, 85, and 18 nM respectively. A K_i value could not be obtained in the nanomolar range for $VO(Im4COO)_2$.

In recent years a variety of PTP-1B inhibitors with a large diversity of chemical structures have been designed for various sites on PTP-1B. Inhibitors can either be designed against the catalytic site (either competitive or non-competitive inhibitors), low affinity binding non-catalytic sites (e.g. site B) or allosteric inhibitors [54-56]. Examples to be considered of both natural and synthetic chemical compounds include vanadate, phenol compounds, oleanolic acid derivatives and sulfathiazole-related compounds as examples as either allosteric or active site inhibitors [57-62]. Various studies on PTP1B inhibitors have found inhibitors, including vanadium-based inhibitors, with K_i values ranging from 3.2 μM – 22nM [54,62]. There are a variety of vanadium inhibitors such as the V(III), V(IV) and V(V) complexes [54]. Vanadate is indicated as a competitive inhibitor (K_i = 0.38 μM) [59] and the mechanism of action has in recent times been proposed to be *via* inhibition of PTPase, and thus counteracting dephosphorylation of the tyrosine phosphate residue of the beta-subunit of the insulin receptor, in such a way restoring the signaling path for cellular glucose intake. In this study we found vanadium salt ($VOSO_4$) to have the lowest K_i (18 nM) and all the other complexes to have K_i values within the nanomolar range and displaying competitive

inhibition, with the exception of $VO(im4COO)_2$. A possible explanation could be the structural rearrangement/decomposition of this complex or that the slight structural difference has not allowed for the optimal orientation of this complex in the active site to optimise the effective inhibition of the hydrogen bonding to be an effect competitive inhibitor [54,56].

3.5.3 Anticoagulation studies

It would be beneficial to create anti-diabetic drugs which simultaneously improve glucose metabolism as well as reduce the hypercoagulable state of diabetic patients. In this study both the extrinsic and intrinsic coagulation pathways were investigated [21,22]. The PT test, APTT assay, D-dimer assay, and the Fib-C test were used to investigate the anti-coagulative effects of the oxidovanadium(IV) complexes [21,22]. The prothrombin time (PT) is the screening test for the extrinsic coagulation pathway. In the PT test, the time required for plasma to clot following conversion of prothrombin to thrombin upon addition of $CaCl_2$ is measured. The activated partial thromboplastin time (APTT) assay investigates the intrinsic pathway. In an APTT reagent, negatively charged particles such as silica are mixed with phospholipids and buffers providing an ideal environment for activation of intrinsic plasma proteins. After incubation of the APTT reagent with plasma, $CaCl_2$ is added which initiates multiple steps of the intrinsic pathway penultimately leading to a fibrin clot. The time from addition of the calcium salt until the clot formation is measured in seconds. In the D-Dimer assay, elevated levels of fibrin reflect a state of activated coagulation and fibrinolysis (hypercoagulation state). The D-Dimer reagent contains latex particles coated with monoclonal antibody specific for the D-Dimer domain of fibrin (soluble fibrin). These D-Dimers are produced when cross-linked fibrin is degraded. In the presence of the D-Dimer reagent these particles agglutinate and the degree of agglutination is directly proportional to the D-Dimer concentration. The Fib-C screening test uses an excess of thrombin to convert fibrinogen to fibrin in diluted plasma. High levels of fibrinogen are usually associated with an increased risk of cardiovascular disease, and the results for the vanadium complexes tested in this study do not alter

the fibrinogen levels and maintain the control levels therefore they would not potentially increase cardiovascular complications. Despite the fact that diabetes mellitus sufferers are usually at a higher risk of thrombotic associated fatalities there has been no investigation into the anti-coagulation potential of the oxidovanadium(IV) complexes before this account.

For the APTT and PT screening tests, only heparin (positive control) significantly increased clotting times relative to the control (Fig. 4). Thus, the oxidovanadium(IV) complexes did not affect either the intrinsic or extrinsic pathways [21,22]. From the Fib-C screening test, it can be seen that $[VO(Im4COO)_2]$ decreased fibrin formation slightly but this was within error of the control (solvent vehicle) and certainly not as significant as the positive control, heparin. From these results, therefore, it is evident that the complexes do not affect either the enzymes playing a role in the intrinsic and extrinsic pathways (as evidenced by lack of inhibition in the PT and APPT tests). They also did not affect the formation of fibrin as seen in the Fib-C test however, the crosslinking required to form a solid clot was inhibited at the concentrations tested as noted by the D-Dimer test. The oxidovanadium(IV) complexes could potentially reduce the hypercoagulation state. However, these results suggested a potential role of vanadium in regulation of the coagulation-thrombolysis process but need to be investigated further.

(Insert Fig. 4 here)

4. Conclusions

Three oxidovanadium(IV) complexes with bidentate imidazolyl-carboxylato ligands were successfully prepared and characterized. Aqueous potentiometric titrations revealed that the incorporation of the low pK_a carboxylic acid group improved the stability of the complexes at low pH values compared to the 2-(2′-hydroxyphenyl)-1*R*-imidazoline ligands presented by us in the literature [52], and other systems with relatively high pK_a hydroxyl groups. The prepared complexes exhibited minimal toxicity in the concentration range tested as well as notable glucose lowering

activity in an *in vitro* assay using muscle, liver and fat cells. The findings from the PTP 1B inhibition studies indicated competitive binding and it is could be speculated that the mechanism of action of the oxidovanadium(IV) complexes could be similar to vanadate, however, this requires further investigation since the complexes could be decomposing and eventually forming vanadate. In addition, there was no significant effect of the complexes for any coagulation tests, with the exception of inhibition of D-dimer formation. Based on the concentrations tested there appears to be potential for the vanadium complexes tested to be able to selectively inhibit the formation of crosslinking of fibrin during its formation from fibrinogen, however these results would need to be completed in a future study using an *in vivo* model. The prepared oxidovanadium(IV) complexes showed potential, and this warrant a further investigation into their anti-diabetic effects using an *in vivo* diabetic rat model.

Acknowledgements

The authors are grateful for financial assistance from the National Research Foundation (NRF-TTK grant) and Medical Research Council (MRC-SIR). We also thank Rhodes University (RU) and Nelson Mandela Metropolitan University (NMMU) for the facilities to carry out this research. We also wish to thank Rudi Nicholas (NMMU) for his assistance with the PTP 1B assays. IZG, RSW and VU are grateful for bursaries received from the Andrew Mellon Foundation, Sasol (Pty) Ltd and Rwanda Education Board, respectively. We thank Dr Adeniyi Ogunlaja for his assistance. We are also grateful to some reviewers for constructive comments.

References

[1] D.O. Abegunde, C.D. Mathers, T. Adam, M. Ortegon, K. Strong, Lancet 370 (2007) 1929-1938.

[2] World Health Organization. Preventing chronic diseases: a vital investment: WHO global report, 2005.

[3] D. Bonnefont-Rousselot, J.P. Bastard, M.C. Jaudon, J. Delattre, Diabetes Metab. 26 (2000) 163-176.

[4] J.A. Meyer, D.M. Spence, Metallomics 1 (2009) 32-41.

[5] W.T. Cefalu, J. Rood, P. Pinsonat, J. Qin, O. Sereda, L. Levitan, R. Anderson, Z.H. Zhang, J.M. Martin, C. Martin, Z.Q. Wang, B. Newcomer, Metabolism 59 (2010) 755–762.

[6] K.H. Thompson, J.H. McNeill, C. Orvig, Chem. Rev. 99 (1999) 2561-2571.

[7] K.H. Thompson, J. Lichter, C. LeBel, M.C. Scaife, J.H. McNeill, C. Orvig, J. Inorg. Biochem. 103 (2009) 554-558.

[8] A. Bordbar, A.L. Creagh, F. Mohammadi, C.A. Haynes, C. Orvig, J. Inorg. Biochem. 103 (2009) 643-647.

[9] D.C. Crans, L. Yang, T. Jakusch, T. Kiss, Inorg. Chem. 39 (2000) 4409-4416.

[10] I.A. Setyawati, K.H. Thompson, V.G. Yuen, Y. Sun, M. Battell, D.M. Lyster, C. Vo, T.J. Ruth, S. Zeisler, J.H. McNeill, C. Orvig, J. Appl. Physiol. 84 (1998), 569-575.

[11] D. Sanna, G. Micera, E. Garribba, Inorg. Chem. 49 (2010) 174-187.

[12] D. Rehder, J. Costa-Pessoa, C.F. Geraldes, M.C. Castro, T. Kabanos, T. Kiss, B. Meier, G. Micera, L. Pettersson, M. Rangel, A. Salifoglou, I. Turel, D. Wang, J. Biol. Inorg. Chem. 7 (2002) 384-96.

[13] M. Passadouro, A.M. Metelo, A.S. Melão, J.R. Pedro, H. Faneca, E. Carvalho, M. Margarida, C.A. Castro, J. Inorg. Biochem. 104 (2010) 987-992.

[14] R. Shukla, R.R. Blonde, Biometals 21 (2008) 205-210.

[15] M. Hiromura, Y. Adachi, M. Machida, M. Hattori, H. Sakurai, Metallomics 1 (2009) 92-100.

[16] K.G. Peters, M.G. Davis, B.W. Howard, M. Pokross, V. Rastogi, C. Diven, K.D. Greis, E.

Eby-Wilkens, M. Maier, A. Evdokimov, S. Soper, F. Genbauffe, J. Inorg. Biochem. 96 (2003) 321-330.

[17] D. Rehder, Met. Ions Biol. Syst. 31, (1995) 1-43.

[18] H. Sakurai, K. Fujii, H. Watanabe, H. Tamura, Biochem. Biophys. Res. Commun. 214 (1995) 1095-1101.

[19] K.H. Thompson, B.D. Liboiron, Y. Sun, K.D.D. Bellman, I.A. Setyawati, B.O. Patrick, V. Karunaratne, G. Rawji, J. Wheeler, K. Sutton, S. Bhanot, C. Cassidy, J.H. McNeill, V.G. Yuen, C. Orvig, J. Biol. Inorg. Chem. 8 (2003) 66-74.

[20] C. Place, J. Zimmermann, E. Mulliez, G. Guillot, C. Bois, J. Chottard, Inorg. Chem. 37 (1998) 4030-4039.

[21] E.W. Davie, K. Fujikawa, W. Kisiel, Biochemistry 30 (1991) 10363-10370.

[22] M.E. Carr, J. Diabetes Complicat. 15 (2001) 44-54.

[23] K.J. Oberhausen, J.F. Richardson, R.M. Buchanan, W. Pierce, Polyhedron 8 (1989) 659-668.

[24] C.C. McLauchlan, J.D. Hooker, M.A. Jones, Z. Dymon, E.A. Backhus, B.A. Greiner, N.A. Dorner, M.A. Youkhana, L.M. Manus, J. Inorg. Biochem. 104 (2010) 274-281.

[25] APEX2, SADABS and SAINT. Bruker AXS Inc.: Madison, WI, USA, 2010.

[26] G.M. Sheldrick, Acta. Cryst. A64 (2008) 112–122.

[27] C.B. Hübschle, G.M. Sheldrick, B. Dittrich, J. Appl. Cryst. 44 (2011) 1281-1284.

[28] G. Gran, Analyst 77 (1952) 661-671.

[29] P. Gans, B. O'Sullivan, Talanta 51 (2000) 33-37.

[30] C. Bazzicalupi, A. Bencini, A. Bianchi, A. Danesi, C. Giorgi, B. Valtancoli, Inorg. Chem. 48 (2009) 2391-2398.

[31] R.P. Henry, P.C.H. Mitchell, J.E.J. Prue, J. Chem. Soc., Dalton Trans. (1973) 1156-1159.

[32] P. Gans, A. Sabatini, A. Vacca, Talanta 43 (1996) 1739-1753.

[33] T. Mossman, J. Immunol. Met. 65 (1983) 55-63.

[34] A.S. Keston, Specific Colorimetric enzymatic analytical reagents for glucose, Abstracts of papers, 129th Meeting American Chemistry Society, Division of biological Chemistry, Dallas, Texas, April 1956, p 31c-32c.

[35] W. Zhang, D. Hong, Y.Y. Zhou, Y.N. Zhang, Q. Shen, J.Y. Li, L.H. Hu, J. Li, Biochim. Biophys. Acta 1760 (2006) 1505 - 1512

[36] APTT Testing. http://us.instrumentationlaboratory.com/products-services/hemostasis-diagnostics/Reagents/General%20Screening%20and%20Anticoagulant%20Monitoring.aspx Date accessed: 11th/ March/ 2014.

[37] P.E. Kleyi, R.S. Walmsley, T.A. Walmsley, I.Z. Gundhla, T. Jauka, J. Dames, R.B. Walker, N. Torto, Z.R. Tshentu, S. Afr. J. Chem. 65 (2012) 231-238.

[38] R.S. Walmsley, Z.R. Tshentu, S. Afr. J. Chem. 63 (2010) 95-104.

[39] G. Wilkinson, R.D. Gillard, J.A. McCleverty, Comprehensive Coordination Chemistry; Elsevier-Pergamon Press: New York, 1987.

[40] T.J. Lane, I. Nakagawa, J.L. Walker, A.J. Kandathil, Inorg. Chem. 1 (1962) 267-276.

[41] A.D. Westland, M.T.H. Tarafder, Inorg. Chem. 20 (1981) 3992-3995.

[42] S.E. Cabaniss, L.F. McVey, Spectrochim. Acta Part A 51 (1995) 2385-2395.

[43] J. Selbin, Chem. Rev. 65 (1965) 153-175.

[44] K. Fukui, H.O. Nishiguchi, H. Kamada, Inorg. Chem. 37 (1998) 2326-2327.

[45] F.H. Allen, Acta Crystallogr.43 B58 (2002) 380–388.

[46] M. Melchior, K.H. Thompson, J.M. Jong, S.J. Rettig, E. Shuter, V.G. Yuen, Y. Zhou, J.H. McNeill, C. Orvig, Inorg. Chem. 38 (1999) 2288.

[47] K. Várnagy, I. Sóvágó, K. Ágoston, Z. Likó, H. Süli-Vargha, D. Sanna, G. Micera, J. Chem. Soc., Dalton Trans. 20 (1994) 2939-2945.

[48] L.D. Pettit, K.J. Powell, Stability constants database-IUPAC and Academic Software, 2007.

[49] D. Sanna, G. Micera, P. Buglyo, T. Kiss, T. Gajda, P. Surdy, Inorg. Chim. Acta 268 (1998) 297-305.

[50] E. Kiss, K. Petrohan, D. Sanna, E. Garribba, G. Micera, T. Kiss, Polyhedron 19 (2000) 55-61.

[51] L. Alderighi, P. Gans, A. Ienco, D. Peters, A. Sabatini, A. Vacca, Coord. Chem. Rev. 184 (1999) 311-318.

[52] R.S. Walmsley, Z.R. Tshentu, M.A. Fernandes, C.L. Frost, Inorg. Chim. Acta 363 (2010) 2215-2221.

[53] M. Passadouro, A.M. Metelo, A.S. Melão, J.R. Pedro, H. Faneca, E. Carvalho, M. Margarida, C.A. Castro, J. Inorg. Biochem. 104 (2010) 987-992.

[54] D. Popov, Biochem. Biophys. Res. Commun. 410 (2011) 377-381.

[55] W.L. Wang, C. Huang, L.X. Gao, C.L. Tang, J.Q. Wang, M.C. Wu, L. Sheng, H.J. Chen, F.J. Nan, J.Y. Li, J. Li, B. Feng, Bioorg. Med. Chem. Lett. 24 (2014) 1889-1894.

[56] J.P. Yin, C.L. Tang, L.X. Gao, W.P. Ma, J.Y. Li, Y. Li, L. Jia, F.J. Nan, Org. Biomol. Chem. 12 (2014) 3441-3445.

[57] J. Zhang, Q. Shen, J.C. Lu, W.Y. Liu, J.J. Yang, J. Li, K. Xiao, Food Chem. 119 (2010) 1491-1496.

[58] Q.C. Liu, T.T. Guo, L. Zhang, Y. Yu, P. Wang, J.F. Yang, Y.X. Li, Eur. J. Med. Chem. 63 (2013) 511-522.

[59] G. Huyer, S. Liu, J. Kelly, J. Moffat, P. Payette, B. Kennedy, G. Tsaprailis, M.J. Gresser, C. Ramachandran, J. Biol. Chem. 272 (1997) 843-851.

[60] Y.B. Tang, D. Lu, Z. Chen, C. Hu, Y. Yang, J.Y. Tian, F. Ye, L. Wu, Z.Y. Zhang, Z. Xiao, Bioorg. Med. Chem. Lett. 23 (2013) 2313-2318.

[61] D. Ye, Y. Zhang, F. Wang, M. Zheng, X. Zhang, X. Luo, X. Shen, H. Jiang, H. Liu, Bioorg. Med. Chem.18 (2010) 1773-1782.

[62] S. Zhang, Z. Zhang-Yin, Drug Discovery Today 12 (2007) 373-381.

Legend of figures

Fig. 1. An ORTEP diagram of **$VO(im4COO)_2 \cdot H_2O$** with ellipsoids drawn at 50% probability level.

Fig. 2. Speciation distribution curves for complexes formed in the ($V^{IV}O$)-imidazole-4-carboxylic acid system (M:L ratio is 1:4).

Fig. 3. The effects of metformin (Met), oxidovanadium(IV) sulfate ($VOSO_4$), [$VO(Im4COO)_2$], [$VO(Im2COO)_2$] and [$VO(MeIm2COO)_2$] (at 1 μM concentration) on Chang, C2C12 and 3T3-L1 glucose uptake. The basal glucose uptake, is represented as 100% (Control). Error bars indicate SEM (n=3), *($p < 0.05$) relative to the (Con).

Fig. 4. The effect of [$VO(Im4COO)_2$], [$VO(Im2COO)_2$] and [$VO(MeIm2COO)_2$] (10 μM) on APTT (A) and PT (B) clotting times, on fibrin formation (C) and D-Dimer formation (D). The control represents untreated sample while the positive control represents the anticoagulant heparin (0.1 $U.mL^{-1}$) (n = 3)

List of Schemes

Scheme 1. The stepwise formation of oxidovanadium(IV) complexes. LH and L^- are omitted in the complexation equilibria for clarity.

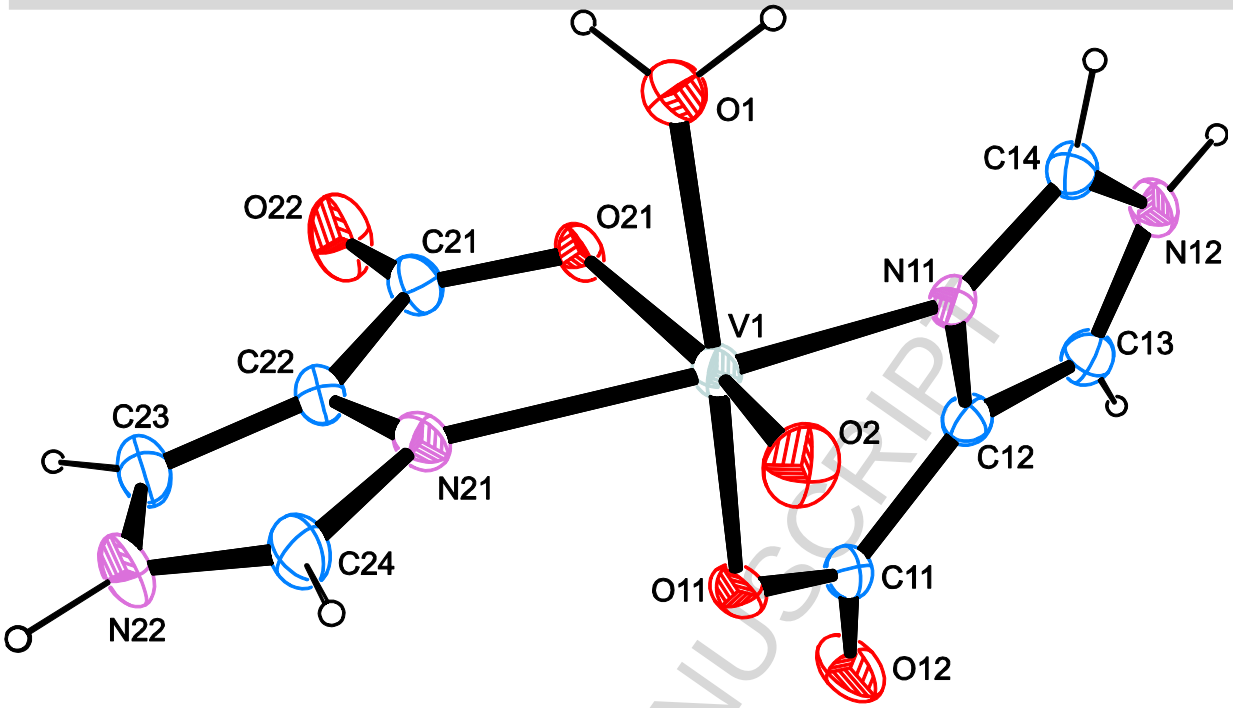

Fig. 1.

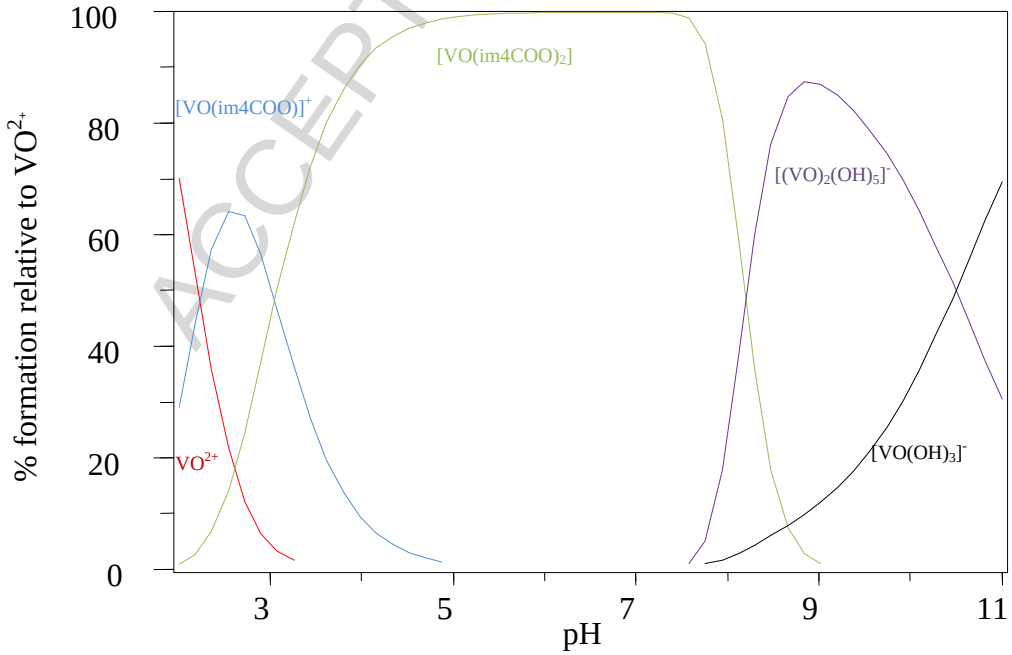

Fig. 2.

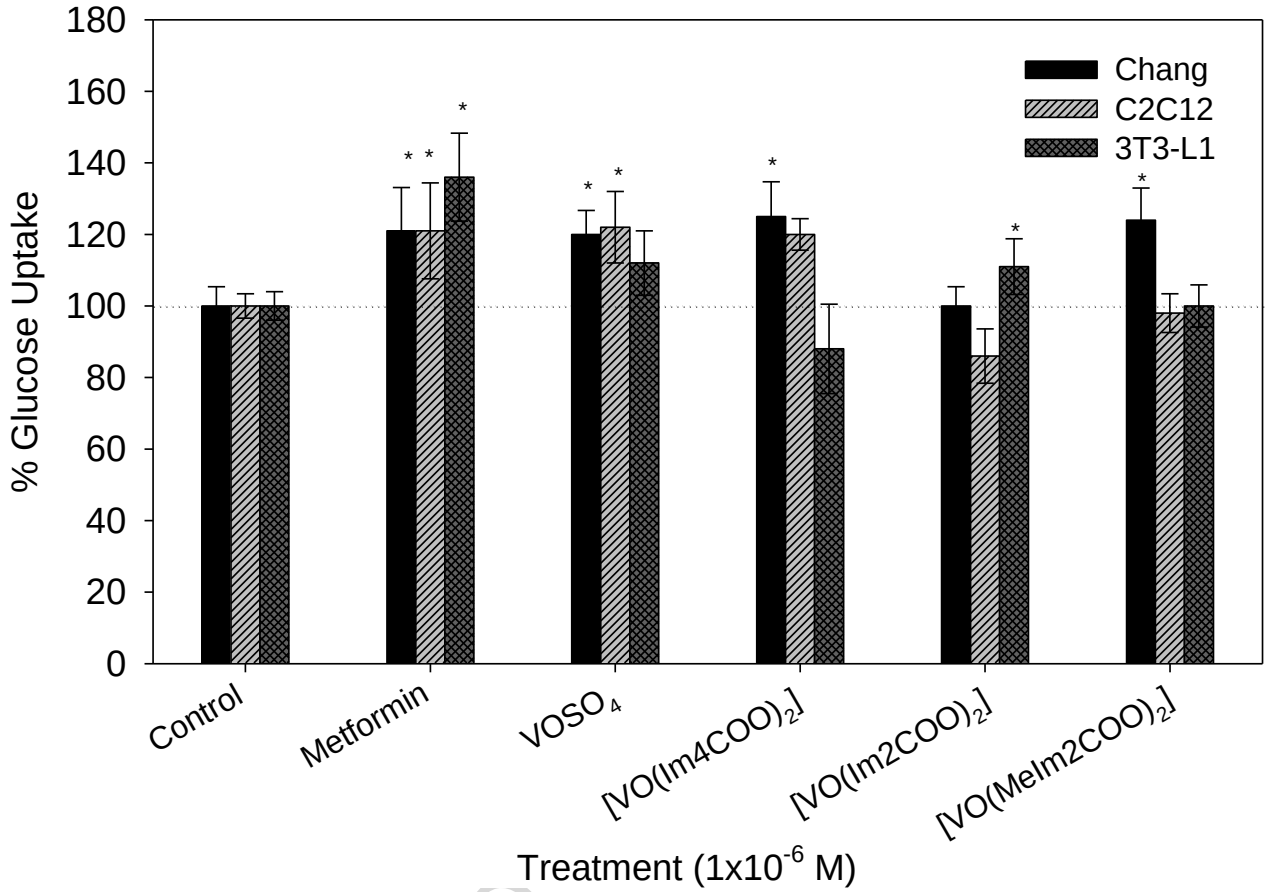

Fig. 3.

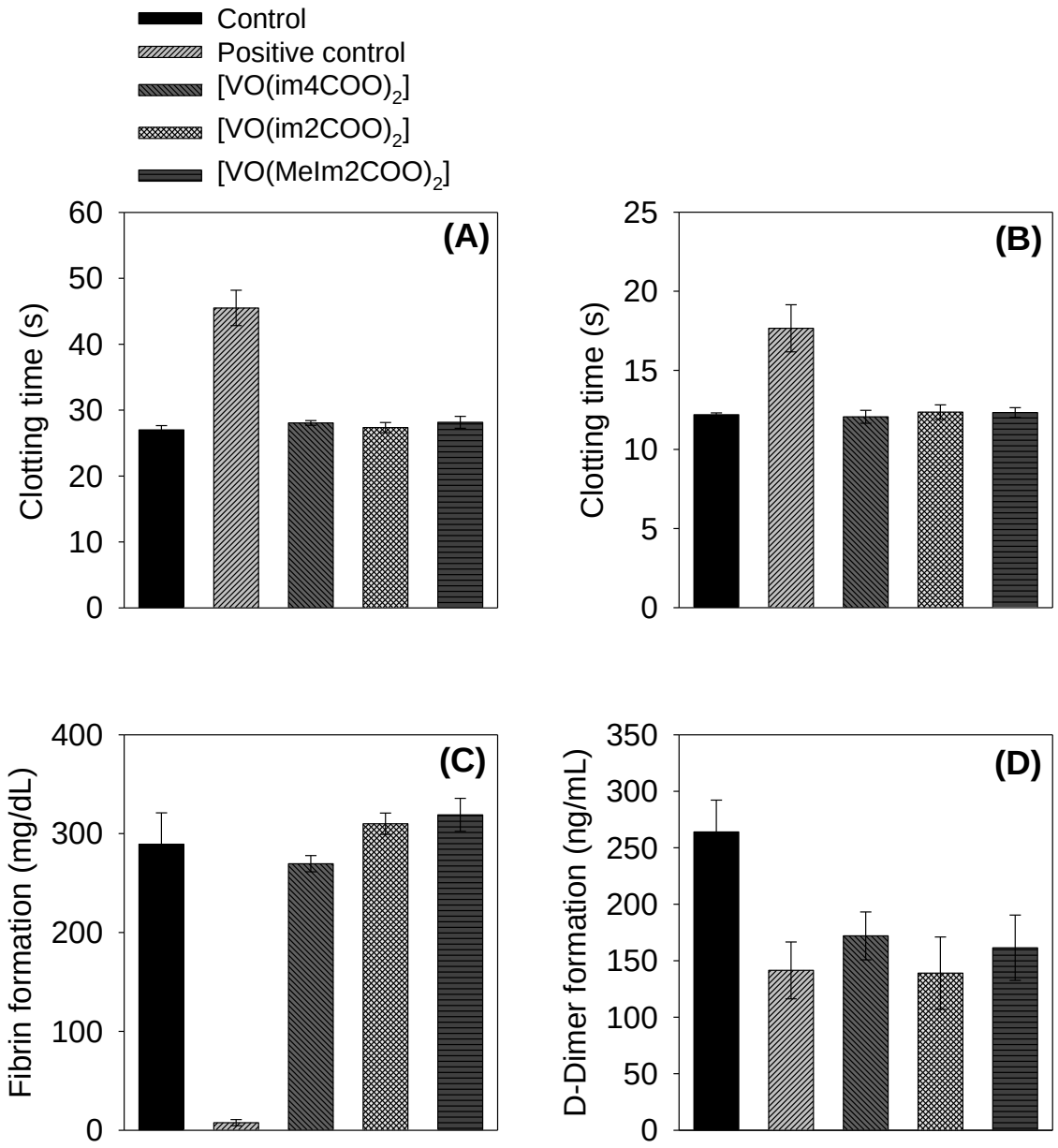

Fig. 4.

List of Schemes

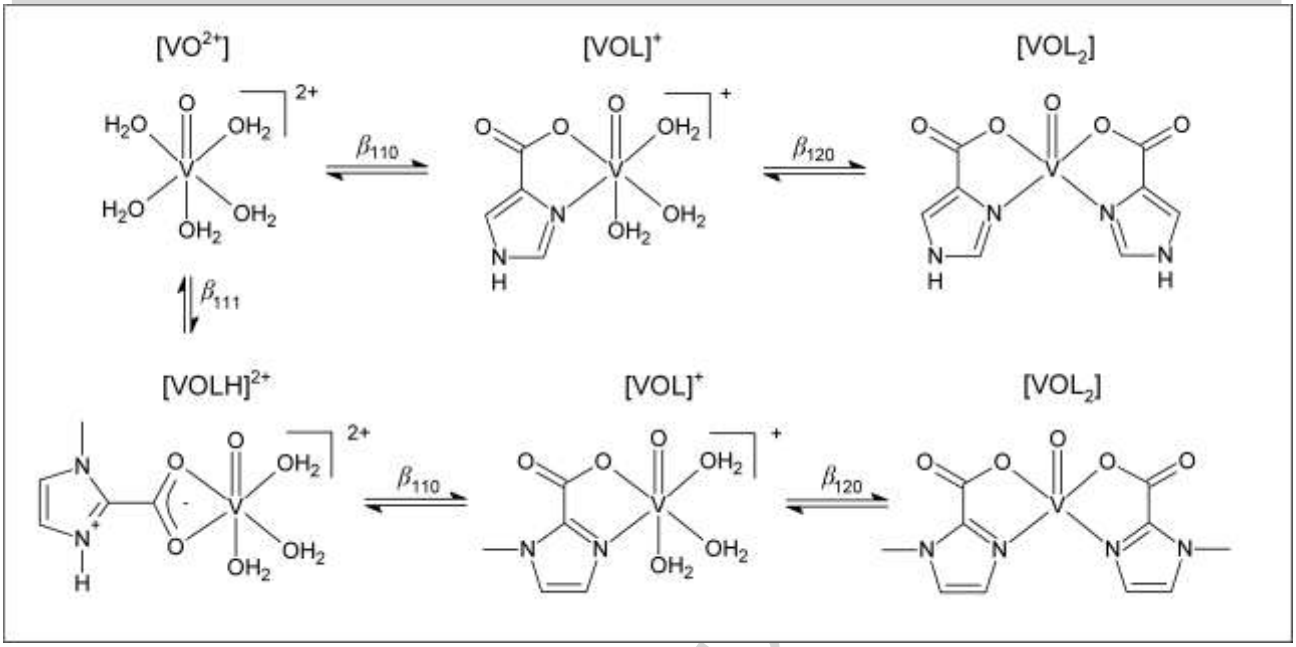

Scheme 1. The stepwise formation of oxidovanadium(IV) complexes. LH and L^- are omitted in the complexation equilibria for clarity.

List of Tables

Table 1. Crystallographic data and structure refinement for **$VO(im4COO)_2 \cdot H_2O$**

Compound	**$VO(im4COO)_2 \cdot H_2O$**
Empirical formula	$C_8H_8N_4O_6V$
Formula weight	307.12
Crystal color	Blue
Crystal system	Monoclinic
Space group	$P2_1/c$
Temperature	200 K
a, Å	13.2735(7)
b, Å	12.0099(8)
c, Å	7.0971(4)
α, deg	90
β, deg	98.082(3)
γ, deg	90
V, Å^3	1120.14(11)
Z	4
ρ_{calc}, g/cm^3	1.821
Wavelength, Å	0.71073
Total reflections	10700
Unique reflections	2774
R	0.0431
R_w	0.1039

Table 2. Selected bond lengths (Å), and angles (˚) for **$VO(im4COO)_2 \cdot H_2O$**

Bond lengths (Å)			
V(1)-O(1)	2.032(2)	V(1)-N(11)	2.080(2)
V(1)-O(2)	1.587(2)	V(1)-N(21)	2.094(2)
V(1)-O(11)	2.023(2)	N(11)-C(14)	1.316(3)
V(1)-O(21)	2.201(2)	N(12)-C(14)	1.341(4)
Bond angles (˚)			
O(1)-V(1)-O(2)	94.97(10)	O(1)-V(1)-O(11)	164.42(8)
O(2)-V(1)-N(11)	100.49(10)	O(2)-V(1)-O(21)	172.23(9)
O(2)-V(1)-N(11)	104.66(10)	N(11)-V(1)-N(21)	155.21(9)
O(2)-V(1)-N(21)	98.45(10)	O(11)-V(1)-N(11)	79.44(8)
N(11)-V(1)-O(21)	82.73(8)	O(21)-V(1)-N(21)	74.67(8)

Table 3. Protonation (log *K*) and stability (log *β*) constants for the $V^{IV}O$-(imidazole,COO) systems at *I* = 0.10 M TMACl and T = 25.0±0.1 °C. Comparison with other $V^{IV}O$-(imidazole/pyridine,COO) systems is also presented. Standard deviations (errors in the last digit) are reported in parenthesis.

	Reaction	Ligand				
		Im-4-COOH	Im-2-COOH	MeIm-2-COOH	Im-4-acetic acid*[49]	Picolinic acid*[50]
pK_1	$LH_2^+ \rightleftharpoons H^+ + LH$	2.70(3)	2.72(3)	1.29(12)	3.19(1)	~1
pK_2	$LH \rightleftharpoons H^+ + L^-$	6.13(1)	6.44(2)	6.75(3)	7.34(1)	5.19(2)
$\log\beta_{110}$	$VO^{2+} + L^- \rightleftharpoons [VO(L)]^+$	7.11(2)	7.53(3)	9.84(6)	6.10(1)	6.66(2)
$\log\beta_{111}$	$VO^{2+} + H^+ + L^- \rightleftharpoons [VO(LH)]^{2+}$	-		14.85(7)	11.04(4)	-
$\log\beta_{120}$	$VO^{2+} + 2L^- \rightleftharpoons [VO(L)_2]$	11.38(8)	11.62(6)	15.49(9)	10.70(1)	12.11(2)

*T = 25.0±0.1 °C and *I* = 0.20M KCl using ca 0.2 M KOH as titrant.

Graphical abstract

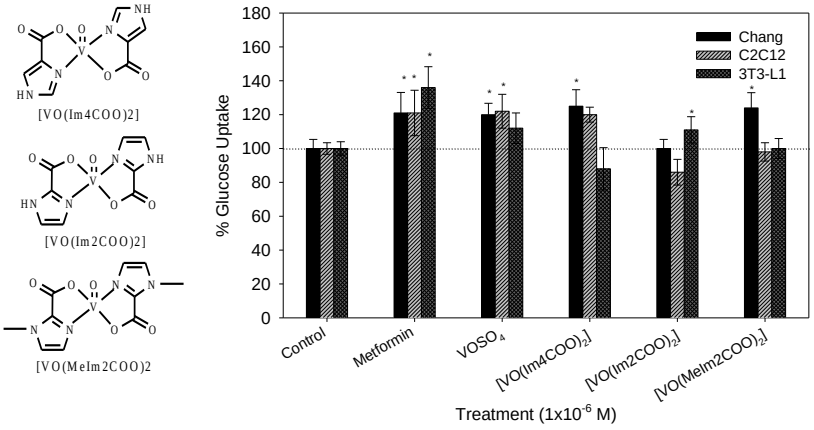

Synopsis for the graphical abstract

The *bis*[(imidazolyl)carboxylato]oxidovanadium(IV) complexes show potential as anti-diabetic agents.

Highlights

- Oxidovanadium(IV) was stabilized by the imidazolyl-carboxylato moiety under physiological pH
- The isolated complexes were shown to activate glucose uptake in cell cultures
- The complexes showed inhibitory effect towards protein tyrosine phosphatase (PTP 1B)
- The complexes also showed inhibition of D-dimer formation